Biophysical Journal Volume 106 April 2014 1701–1709

Water-Peptide Site-Specific Interactions: A Structural Study on the Hydration of Glutathione

Ernesto Scoppola,[†] Armida Sodo,[†] Sylvia E. McLain,[‡] Maria Antonietta Ricci,[†] and Fabio Bruni[†*]

[†]Dipartimento di Scienze, Università degli Studi di Roma Tre, Via della Vasca Navale 84, 00146 Roma, Italy; and [‡]Department of Biochemistry, University of Oxford, South Park Road, Oxford, Oxfordshire OX1 3QU

ABSTRACT Water-peptide interactions play an important role in determining peptide structure and function. Nevertheless, a microscopic description of these interactions is still incomplete. In this study we have investigated at the atomic scale length the interaction between water and the tripeptide glutathione. The rationale behind this work, based on the combination between a neutron diffraction experiment and a computer simulation, is twofold. It extends previous studies on amino acids, addressing issues such as the perturbation of the water network brought by a larger biomolecule in solution. In addition, and more importantly, it seeks a possible link between the atomic length scale description of the glutathione-water interaction with the specific biological functionality of glutathione, an important intracellular antioxidant. Results indicate a rather weak hydrogen bond between the thiol (-SH) group of cysteine and its first neighbor water molecule. This -SH group serves as a proton donor, is responsible for the biological activity of glutathione, and it is involved in the formation of glutathione disulfide, the oxidized form of glutathione. Moreover, the hydration shell of the chemically identical carboxylate group on the glutamic acid residue and on the glycine residue shows an intriguing different spatial location of water molecules and coordination numbers around the two CO_2^- groups.

INTRODUCTION

Water-protein interactions have long been considered essential in determining protein structure and function in vivo (1,2). Although there has been much progress on understanding hydration of specific amino acid residues in fully folded proteins by the combination of NMR and/or x-ray crystallography coupled with molecular dynamics (MD) simulations (3–7) a complete microscopic description of the interactions between water atoms and specific sites of the peptide backbone and its side chains is still sparse. A description at the atomic scale of water hydration can provide insights on still open and important issues such as protein folding and association as well as protein-ligand binding, where water-related interactions have been proposed to dominate the thermodynamic signature of molecular recognition in ligand binding (6). To date, investigations concerning site-specific water-protein interactions in solution at the atomic length scale have coupled spectroscopic measurements with computation to understand which residues are preferentially interacting with the surrounding water solvent (3,4). Although NMR is a powerful tool for probing the structure of small peptides in solution, important details of the water hydration are lost on the time scale of NMR as it gives a spectral average of the water signal or any hydrogen binding site that is in fast exchange with the surrounding water solvent. Moreover, even when waters exhibit long residency times at certain sites, which have been observed by two-dimensional-NMR techniques, details of specific water-hydrogen bonding interactions are difficult to determine (3).

Significant progress has been recently made by combining neutron diffraction techniques with computer simulations to unveil structural information on water interactions with single amino acids or dipeptides at an unparalleled level of detail at the atomic length scale (8–12) *in solution*. Analogous to crystallography, where atomic level interactions can be determined, the advantage of this approach is attributable to the ability of extracting pair-wise atomic interactions. Additionally, structural measurements of molecules in solution provides details of interactions between the biomolecule and the surrounding water solvent in the physical medium where most of these interactions take place in vivo, thus providing a microscopic description of the structure and coordination of water molecules near the biomolecular functional groups.

In particular, a better understanding of specific side chain hydration could help to clarify the often stated argument on hydration water (namely water molecules in the first hydration shell of a biomolecule) being different, with regard to structural and dynamical properties, from bulk water (1,2,13,14). It should be noted that there is sparse quantitative evidence, and even some disagreement, on the difference at an atomic scale length (0 to 10 Å), between bulk and hydration water. Neutron diffraction experiments, combined with computer modeling, offer important advantages over other techniques, as they provide a direct and detailed set of structural information unobtainable with other experimental approaches. Details of the solvent water structure in biomolecular solutions also may give clues into biological processes in solution. For instance, previously investigated

Submitted September 3, 2013, and accepted for publication January 31, 2014.

*Correspondence: fabio.bruni@uniroma3.it

Editor: Josh Wand

0006-3495/14/04/1701/9 $2.00

http://dx.doi.org/10.1016/j.bpj.2014.01.046

dipeptides have an electrostrictive effect on water, although this effect has not been observed in similar experiments on the amino acid L-proline in solution, even though proline is a constituent of two of the previously measured dipeptides (9,10). This electrostrictive effect has been shown to be attributable to the addition of charged solutes to water, and is similar to the effect of external pressure applied to pure water. This effect is observed as a shift toward smaller distances of the position of the second peak of the water oxygen-oxygen radial distribution function (15–18). The comparison between the effect of amino acids and dipeptides on water suggests there are other effects besides charge influencing solvent properties; long-ranged perturbation on the water network caused by the presence of a dipeptide in solution could also be a determining factor. As a consequence, it could be speculated that the electrostriction of the water network is one of the preliminary steps in protein and peptide folding in solution (10).

In the present study we have investigated, at the atomic scale length, the structural interactions between water and the tripeptide glutathione (GSH) in solution. The rationale behind this work, is twofold. On one hand, it extends previous studies on amino acids and dipeptides, addressing issues into the perturbation of the water network brought by the presence of a larger biomolecule in solution. On the other hand, and importantly, it seeks a possible link between an atomic length scale description of the glutathione-water interaction with the specific biological functionality of this tripeptide, an important intracellular antioxidant. Glutathione has a $\gamma-$ peptide linkage between the amine group of cysteine and the carboxyl group of the glutamate side-chain (see Fig. 1).

In particular, the thiols (-SH) in cysteine residues within proteins are among the most susceptible oxidant-sensitive targets and can undergo various reversible and irreversible redox alterations in response to oxidative stress. The varieties of protein thiols can potentially affect protein activity, thus leading to the impairment of many cell functions (19). Glutathione is present in almost all mammalian and plant cells at millimolar concentrations, where it is found in its reduced form (GSH) and in its oxidized form, glutathione disulfide (GSSG) (20). This is the product of the reaction between two GSH molecules, now linked through their thiols groups, and the ratio of GSH to GSSG is critical to cellular redox balance. Changes in the cell redox status (mainly because of a decrease in the GSH/GSSG ratio and/or depletion of GSH by the metabolism of drugs) may induce reversible formation of mixed disulfides between protein sulfhydryl groups and glutathione on multiple proteins, which makes of cellular glutathione a crucial modulating factor for an ever-increasing number of proteins (19,20). Therefore, a detailed description of the interaction between water molecules and specific glutathione groups, in particular its thiol, is a key factor in unveiling the mechanism of glutathione conversion to its oxidized form. In this study, we test the feasibility of our approach, by looking at

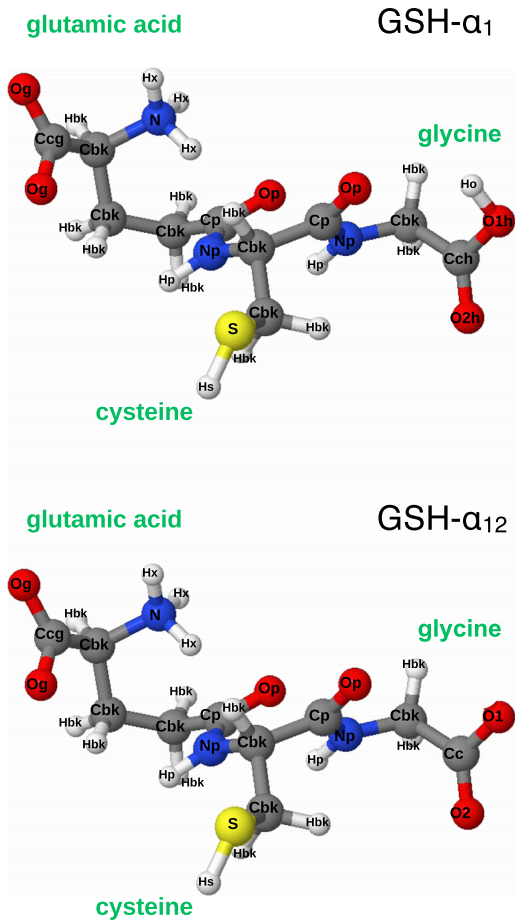

FIGURE 1 Molecular structure of the tripeptide glutathione (GSH) in its protonation state α_1 (*top*), and α_{12} (*bottom*). GSH-α_1 and GSH-α_{12} represent, respectively, the 60% and 30% of the possible states of GSH at the investigated pH $\sim$ 3. Each atom site has been labeled according to the symbols used in the EPSR simulation, see Table S2 in the Supporting Material. To see this figure in color, go online.

concentrated glutathione solution at a low pH $\sim$ 3. This choice is dictated by two factors: first, the relatively high peptide concentration (compared with intracellular glutathione concentration) ensures a relatively large signal due to the peptide compared with that of the solvent, underlining the likely effect of this solute on water structure. Second, the low pH is a result of dissolving of glutathione in water in the absence of buffer. Adding buffer to increase the pH to physiological values requires the addition of other solutes to the GSH solution. The absence of extra chemical species, beside peptide and water, in the sample ensures that the system is as simple as possible and that only the glutathione-water interactions will be addressed without complications from additional solute molecules.

MATERIALS AND METHODS

Glutathione ($C_{10}H_{17}N_3O_6S$, $\gamma-$ L-glutamyl-L-cysteinylglycine) was purchased from Sigma-Aldrich (Milan, Italy) (CAS 70-18-8) and used without

further purification. Aqueous solutions investigated by neutron diffraction experiments, were prepared at a concentration corresponding to 1 solute molecule per 130 water molecules (~ 0.42 M), where the measured pH of this solution was 3.0 (pH measured with a Hanna Instrument (Smithfield, RI) pH 211). Deuterated samples were obtained by lyophilizing glutathione in D_2O to replace the exchangeable hydrogens of the tripeptide with deuterium; this procedure was repeated several times to obtain a full isotopic substitution of the exchangeable hydrogens. Deuterated glutathione solutions were then prepared using deuterated glutathione in D_2O. Neutron diffraction experiments have been performed using the SANDALS neutron diffractometer, installed at the ISIS Facility (Harwell Oxford, UK) (21). To fully exploit the advantages of isotopic substitution, a set of isotopically labeled samples were prepared (see Table S1 in the Supporting Material).

Data have been collected also for the empty instrument, empty container, and vanadium standard, to normalize the data for all investigated samples to an absolute scale. Diffraction data have been processed using the "Gudrun" suite of programs (22,23), which performs corrections for multiple scattering, absorption, inelasticity effects, and scattering from the samples. "Gudrun" also verifies that the measured scattered intensity is consistent with sample density and composition.

The outputs of "Gudrun" are the total neutron-weighted interference differential cross sections (IDCS) defined as follows:

$$F(Q) = \sum_{\alpha} \sum_{\beta \geq \alpha} w_{\alpha\beta}[S_{\alpha\beta}(Q) - 1] \quad (1)$$

where α and β label the atomic sites; and Q is the magnitude of the change in the momentum vector by the scattered neutrons, defined as $Q = 4\pi\, sin\theta/\lambda$, where 2θ represents the scattering angle and λ represents the wavelength of scattered radiation. The following functions

$$S_{\alpha\beta}(Q) = 4\pi\rho \int_0^{\infty} r^2 \left(g_{\alpha\beta}(r) - 1\right) \frac{\sin Qr}{Qr} dr, \quad (2)$$

called partial structure factor (PSF), are the Fourier transforms of individual site-site radial distribution function $g_{\alpha\beta}(r)$, and ρ is the atomic number density of the solution. The individual PSFs are weighted in Eq. 1 by $w_{\alpha\beta} = c_\alpha c_\beta b_\alpha b_\beta (2 - \delta_{\alpha\beta})$, where c_α and c_β are the concentrations of the α and β nuclei, and b_α and b_β are their scattering lengths (24), respectively.

Thus, each experimental IDCS is a linear combination of many PSF of the individual site-site radial distribution functions. In liquids with a small number of distinct atoms, such as H_2O, by measuring an array of different isotopically labeled samples, it is possible to directly extract all of the pair correlation functions from the experiment, giving a direct assessment of the hydrogen bonding present in the measured liquid. However, in more complex samples, such as those investigated in the present report, it is not possible to isotopically label every atomic site; for this reason, we employ a simulation-assisted procedure that has been developed to convert IDCS data to real space, and extract a whole set of radial distribution functions. This is called empirical potential structure refinement (EPSR) (25,26) and is similar in principle to the methods routinely used in crystallography, which attempt to systematically refine a structural model to give best overall agreement with the diffraction data. Moreover, it should be noted that the larger is the number of isotopic contrast samples measured, the larger the number of constraints for the EPSR procedure; EPSR is required to fit all of the data sets, ensuring a physically reasonable model that is consistent with a set of measured diffraction data at the appropriate density and composition of each sample. The EPSR computational model has been extensively used and tested for about two decades on many disordered materials. Although EPSR does not necessarily provide the only possible interpretation of the structural data, it does provide a model that is consistent with the measured diffraction data. More detailed descriptions and discussions on the potential limitations, uniqueness of the EPSR results, and its comparison with standard Monte Carlo techniques can be found elsewhere in the literature (27–29). Details on the EPSR procedure, as applied in the present study, EPSR reference potential parameters, and the comparison between measured data and those reproduced by the EPSR method are shown in the Supporting Material.

In the present study, in an aqueous solution of glutathione at pH 3.0, the tripeptide can be found in four different protonation states (30). Two of these are most relevant as together they represent the 87% of the possible states of glutathione. These two species, labeled GSH-α_1 and GSH-α_{12}, respectively, are in the zwitterionic form but the carboxylic group of glycine is protonated on GSH-α_1 and deprotonated on GSH-α_{12} (Fig. 1).

The other two GSH species, not considered here for the sake of simplifying the simulation box, are GSH-α_0, with all terminal groups protiated, and GSH-α_2, with a deprotonated carboxylic group on glutamic acid. These two latter species represent, respectively, the 8% and 5% of the possible states of GSH. Clearly, the EPSR simulation box must include GSH-α_1 and GSH-α_{12} to represent a realistic but simple model of the investigated sample. In addition, it is important to know whether at pH 3 and at the investigated concentration, reduced (GSH) and oxidized (GSSG) glutathione could both be present (GSSG is made of two GSH molecules covalently bound through S-S linkages). This possibility has been tested with a preliminary Raman spectroscopy experiment on our samples. Raman spectra indicated no vibrational peak due to S-S bridge, and the characteristic peak of the S-H group was clearly visible. Therefore, the presence of GSSG can be safely excluded, and the EPSR simulation box includes only GSH, in two protonation states, and water molecules.

RESULTS AND DISCUSSION

As shown in the Supporting Material, the measured diffraction data and the EPSR fits are in very good agreement (Fig. S1); this ensures that the simulation box is indeed a good model of the real sample. Information not accessible experimentally can be thus extracted from the simulation box and discussed in the following.

Water-water interactions

Fig. 2 shows the radial distribution functions (RDFs) for water sites (H_w, O_w) from the glutathione solutions, compared with those obtained for pure water (31).

The comparison between the RDFs of water as a solvent and pure water shows small differences both regarding the peak positions and their amplitude. This indicates that there is no appreciable change in the pure water structure upon the addition of GSH. The largest difference can be observed considering the O_w-O_w RDF; this is not surprising given the high sensitivity of the O-O correlation function to any perturbation to pure water (pressure, temperature, presence of solutes, etc.) (32). In particular, it has been shown that the presence of some solutes results in a shift toward smaller distances of the second peak of the oxygen-oxygen RDF (16,17). Fig. 2 shows that no such shift can be observed for water molecules solvating GSH, in comparison with pure water (see insert Fig. 2). Peaks of the O_w-O_w RDF, and in particular the second one, are less intense for water in GSH solutions, compared with pure water, thus indicating a larger degree of orientational disorder due to the presence of GSH, but peak positions are unchanged compared with pure water. The position of the second peak of the oxygen-oxygen RDF, centered at 4.5 Å is usually taken as the signature for the tetrahedral water coordination. The

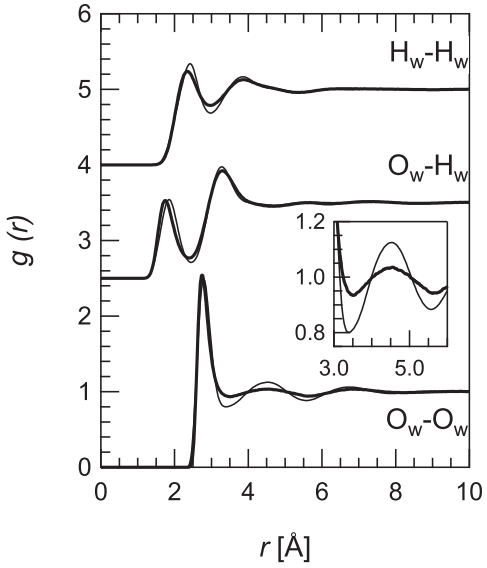

FIGURE 2 Site-site radial distribution function of water sites, O_w and H_w, for water as a solvent (*thick solid lines*) compared with pure water (*thin solid lines*). The insert shows the region around the second peak of the O_w-O_w. The peak position is unchanged, compared with pure water, indicating that the solute GSH does not alter average water structure.

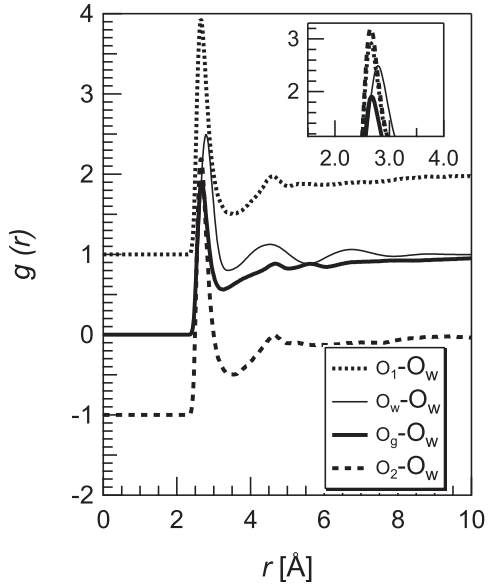

FIGURE 3 Site-site radial distribution function of water oxygen O_w around the oxygens of the glutamic acid, O_g, and the oxygens on the glycine, O_1 and O_2 for GSH-α_1, see Fig. 1. The O_w-O_w radial distribution function for pure water is also shown as a thin solid line for comparison. The insert shows the region of the first peak of all the plotted radial distribution functions (RDFs), indicating a clear shift to smaller distances of its position for the O_g-O_w, O_1-O_w, and O_2-O_w RDFs, in comparison with pure water. All glutathione-water RDFs show a slope, that is the signature of excluded volume effects, because of the large size of the tripeptide compared with that of a water molecule.

observation that the presence of GSH does not alter water coordination is quite puzzling, as similar previous experiments on dipeptides in water reported a clear shift of the second peak position (10), whereas proline in solution resulted in a virtually unchanged O_w-O_w second peak position (9), similar to the present results. Even though the solute concentration in these previous studies is higher compared with that of GSH it could have been reasonable to predict a shift of this peak due to the presence of GSH, given its size and structure.

Water-carboxylate group interactions

As stated above, the pH of the aqueous GSH solution investigated is 3.0. As a consequence, there are two GSH species present in the sample and in the EPSR simulation box, GSH-α_1 and GSH-α_{12}, differing with respect to their protonation states. Specifically, there is a -CO_2^- group on the glutamic acid residue of both GSH species, whereas in GSH-α_1 the glycine carboxylate group is protonated (-COOH) and deprotonated (-CO_2^-) in GSH-α_{12}, where GSH-α_{12} represents the 30% of all glutathione molecules in the simulation box. Fig. 3 shows the radial distribution function for the water oxygens around the terminal oxygens of the -CO_2^- group on glutamic acid, labeled as O_g in Fig. 1.

These two oxygen sites are considered as equivalent in the EPSR simulation (see Table S2). Similar RDF are also shown in Fig. 3 for the two oxygen sites, labeled as O_1 and O_2, belonging to the -CO_2^- group on GSH-α_{12} glycine residue. The RDF for water oxygen around the terminal oxygens of the carboxylate groups on GSH show relatively small differences to each other, such as a larger orientational disorder, as indicated by the slightly broader peak around 4.5 Å, and the presence of a small feature at ~ 6 Å for water oxygen around O_g compared with the other oxygen sites. Conversely, there are significant differences in comparison with the RDF of water oxygen, O_w-O_w. In particular, the position of the first peak is shifted to smaller distances compared with that of pure water (it moves to 2.65 Å for the -CO_2^- groups compared with 2.75 Å, insert of Fig. 3), and the second and third peaks are less defined or absent, than is the case of pure water.

Fig. 4 shows the radial distribution function of water hydrogens around the O_g site. The first peak in the O-H RDF is indicative of a hydrogen bond, and, interestingly, water-terminal O_g hydrogen bonds, compared with the H-bonding peak in pure water are slightly shorter as the H-bond peak moves from 1.80 Å in pure water to 1.68 Å for water molecules in the O_g hydration shell.

These results suggest the presence of stronger interactions between water molecules and electronegative sites on the peptide (the -CO_2^- is a hydrogen bond acceptor), compared with pure water, likely because of the presence of the partial charge on carboxylate group. The coordination numbers for water-carboxylate groups are listed in Table 1.

These are calculated considering all water molecules within a distance of 3.5 Å from a oxygen site of a carboxylate

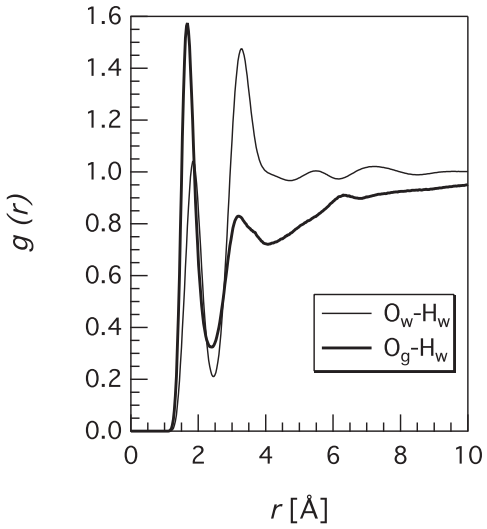

FIGURE 4 Site-site radial distribution function of water hydrogen, H_w, around the oxygens of the glutamic acid, O_g (*thick solid line*). For the sake of comparison, the O_w-H_w is also plotted as a thin solid line. The first peak, usually taken as the signature of the H-bond, is slightly shifted to smaller distances for O_g-H_w, suggesting the presence of shorter and possibly stronger H-bonds between water and O_g sites of glutathione. Excluded volume effects, because of the large size of the tripeptide, compared with that of a water molecule, are visible for the plotted O_w-H_w RDF.

group; this distance corresponds to the first minimum of the RDF shown in Fig. 3. Interestingly, there is a noticeable difference between the number of water molecules in the first hydration shell around the different carboxylate groups, with less than five water molecules hydrating the -CO_2^- site on the glutamic acid, and more than seven water molecules hydrating the -CO_2^- on the glycine.

To better visualize the differences between the hydration pattern around the glutathione carboxylate groups, the spatial distribution function (SDF) for water oxygen around the different carboxylate groups, namely that of the glutamic acid residue (panel A), and that of glycine residue (panel B) are shown in Fig. 5. These SDFs show the probability of finding a water molecule around a -CO_2^- group, for the average structure in solution.

TABLE 1 Coordination numbers of water molecules in the hydration shell of specific groups on the glutathione molecule

Atomic site	Coordination number
Glutamic acid	
O_g	2.35
H_x	1.01
Glycine	
O_1	3.57
O_2	3.86
O_{1h}	1.37
O_{2h}	2.42
Cysteine	
H_s	0.64

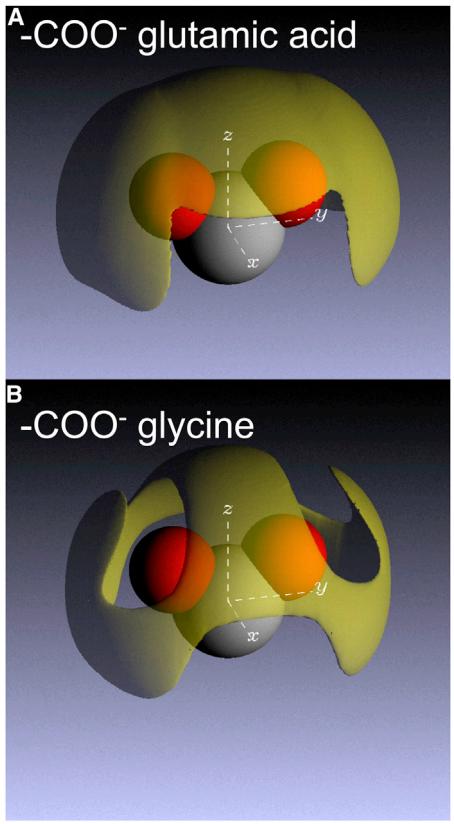

FIGURE 5 Spatial density functions (SDF) showing the distribution of water molecules around the -CO_2^- group on glutamic acid (*A*), and around the -CO_2^- group on glycine (*B*). The yellow shaded areas represents regions where there is a probability of finding a water molecule at a distance range 2.00 to 4.47 Å (*A*) or at a distance range 2.00 to 4.26 Å (*B*) from the central carbon atom. These distance ranges correspond to the first coordination shell of the C_{cg}-O_w RDF, and of the C_c-O_w RDF, respectively (data not shown), where C_{cg} is the carbon atom of the -CO_2^- group on glutamic acid, and C_c is the carbon atom on glycine (see Fig. 1). The plotted SDFs show 65% of the water molecules within the ranges indicated. To see this figure in color, go online.

In both panels, the carbon atom is at the origin of the reference frame and the oxygens are in the $yz-$ plane. The yellow regions indicate regions where the probability of finding a water molecule is higher than a set threshold value (see legend to Fig. 5). Full details of the procedure required to calculate these SDF are described elsewhere in the literature (see for instance (8) and references therein). The comparison between -CO_2^- in Fig. 5 is quite striking, as there is an almost uniform hydration pattern around the glutamic acid -CO_2^- group (panel A). Conversely, the presence of preferred locations, along with regions showing the absence of water density, for water molecules around the -CO_2^- group on the glycine residue (panel B). A direct comparison between these findings and those obtained in previous studies on single amino acids (8,9) and on the amino acid glutamine (11) is not straightforward, given the difference in solute size and concentrations, and threshold value adopted to calculate the SDFs. Nevertheless, it is reasonable

to state that the hydration shell shown in Fig. 5 *A* and *B* are broadly consistent with previous results on the hydration of -CO_2^- groups in solution. They all show preferred locations of the water molecules above the group (in the positive $z-$ direction), as well as in a region in the $+y$ and $-y$ directions. However, what is striking here is that the two carboxylate groups of glutathione CO_2^- groups have clearly distinct hydration shells. This observation indicates a different solvent accessibility of -CO_2^- groups depending on their location within the same molecule; water molecules show no obvious preferred orientations or positions when hydrating the glutamic acid residue carboxylate group that is situated next to an -NH^{3+} group. This hydration shell is somewhat similar the -CO_2^- group hydration observed for glutamine (11) which is also located next to an -NH^{3+} group. Although -CO_2^- group hydration of glutamate in solution at the same position does show preferred locations of surrounding water molecules in the first hydration shell, in that work only the very nearest neighbor molecules were plotted (in a distance range of 0-3.5 Å (8)). Conversely, preferred orientations and positions of water molecules are found around a carboxylate group next to a -CH_2, as in GSH. The different -CO_2^- hydration shells determined for glutathione may provide a way for water to "identify" specific peptide sites, and, more generally, the different hydration pattern of specific groups on amino acids and peptides might play a role in the early stages of protein folding, and on functionality of these molecules in solutions. It should be noted that SDFs, such as those depicted in Fig. 5, show the probability, above a set threshold, to find a water molecule around specific solute groups in solution. Therefore, they provide structural information that is ensemble- and time-averaged, as neutron diffraction measurements yield details of the ensemble and time average of the investigated solution. As a result, dynamical processes such as solvent fluctuations and also bulk thermodynamic quantities cannot be easily assessed from the EPSR model of the neutron diffraction data.

Water-carboxylic acid group interactions

The investigated peptide solution, and consequently the EPSR simulation box, contains also the protonated GSH-α_1, representing 70% of all the glutathione molecules in the present solution, where the glycine peptide of GSH-α_1 has a carboxylic group (-COOH) at the investigated pH. Fig. 6 shows the radial distribution function of the carboxylic oxygens, O_{1h} and O_{2h} (see Fig. 1) with water oxygens, O_w. For the sake of comparison, the O_w-O_w is also shown in Fig. 6. With regards to the position and intensity of the first peak (see insert in Fig. 6), this peak is either in the same position as that of pure water (2.76 Å, for the O_{2h}-O_w RDF), or it is shifted to a larger distance (2.85 Å, for the O_{1h}-O_w RDF). The intensity of the first peak is sensibly reduced in comparison with that of pure water, resulting in relatively small coordination numbers (Table 1): there are less than four water molecules hydrating the carboxylic group on GSH.

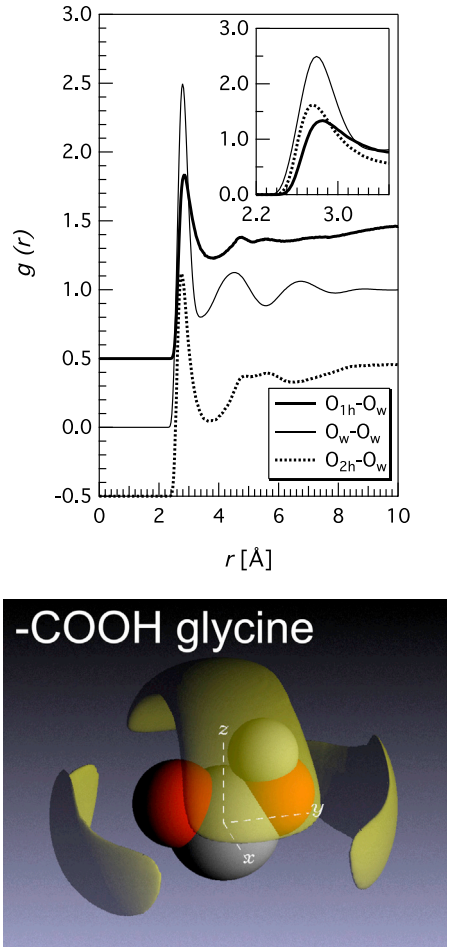

FIGURE 6 Top panel: site-site radial distribution function of water oxygen O_w around the oxygens, O_{1h} and O_{2h}, of the carboxylic group of glycine in the GSH-α_{12} protonation state, see Fig. 1. The O_w-O_w radial distribution function for pure water is also shown as a thin solid line for comparison. The insert shows the region of the first peak of all the plotted RDFs, indicating a slight shift to a larger distance of its position for the O_{1h}-O_w, whereas there is no change and O_1-O_w, and no variation of its position for O_{2h}-O_w RDFs, in comparison with pure water. Bottom panel: spatial density functions (SDF) showing the distribution of water molecules around the -COOH group on glycine in the GSH-α_{12} protonation state, see Fig. 1. The yellow shaded areas represents regions where there is a probability of finding a water molecule at a distance range 2 to 4.44 Å from the central carbon atom. This distance range corresponds to the first coordination shell of the C_{cch}-O_w RDF (data not shown), where C_{cch} is the carbon atom of the -COOH group on glycine (see Fig. 1). The plotted SDFs show 65% of the water molecules within the ranges indicated. To see this figure in color, go online.

All these observations are consistent with the presence of the terminal hydrogen atom bound to O_{1h} site and with the smaller charge on both O_{1h} and O_{2h} in comparison with O_1 and O_2 (see Table S2 and Fig. 3 for comparison with the carboxylate group). Therefore, it is reasonable to state that water molecules are less tightly bound to the carboxylic

group in comparison with the carboxylate group. The spatial distribution of water molecules around the -COOH group is visualized in Fig. 6.

Compared with Fig. 5 panel B, the location of water molecules around the carboxylic group shows preferred location and a larger degree of directionality. Water molecules are more likely placed on top of the -COOH group and on the sides of the carboxylic oxygens. As expected, the presence of large void regions is consistent with the smaller coordination numbers of water molecules in the hydration shell of this peptide site.

Water-amine group interactions

There is a -NH^{3+} group bound to the glutamic acid on both GSH species (see Fig. 1). Fig. 7 shows the radial distribution function around the amine group, and, in particular, the RDF of water oxygens, O_w, with each of the hydrogen sites on the -NH^{3+} group: these are labeled as H_x.

The amine group is an hydrogen bond donor, and the first peak of the RDF plotted in Fig. 7, indicates shorter and possibly stronger hydrogen bonds between the amine group and surrounding water molecules, compared with the case of pure water (see insert of Fig. 7). The sloping trend of the H_x-O_w RDF for r>4 Å is attributable to the presence of regions where water molecules are not allowed (excluded volume effects). This effect can be observed in all the RDFs shown previously, but it is more evident in Fig. 7. Correction for this effect (16), resulting in a RDF with oscillations around unity, is not trivial, as it requires a detailed knowledge of the structure factor of the peptide molecule. Table 1 lists the coordination numbers of water molecules in the hydration shell of the amino group: there are three water molecules hydrogen bonded to this protein site, one for each H_x atom. The spatial distribution of these water molecules is shown in Fig. 7: the hydration shell has a ribbon-like conformation around the -NH^{3+} group, with a high probability of finding a water molecule with its oxygen directly facing each of the three H_x sites.

The region on top of the amino group is not occupied by water molecules in the first hydration shell of this protein site. The hydration pattern around the amino group determined in the present study is in good agreement with that found for the backbone -NH^{3+} group of glutamine (11).

Water-thiol group interactions

The peptide cysteine, one of the three building blocks of GSH, has a thiol residue, namely a -SH group that is highly reactive. This is the site where two GSH molecules can be linked through a S-S bond making GSSG, the oxidized form of glutathione. Fig. 8 shows the radial distribution function of water oxygen around the hydrogen site of the -SH group, labeled H_s (Fig. 1).

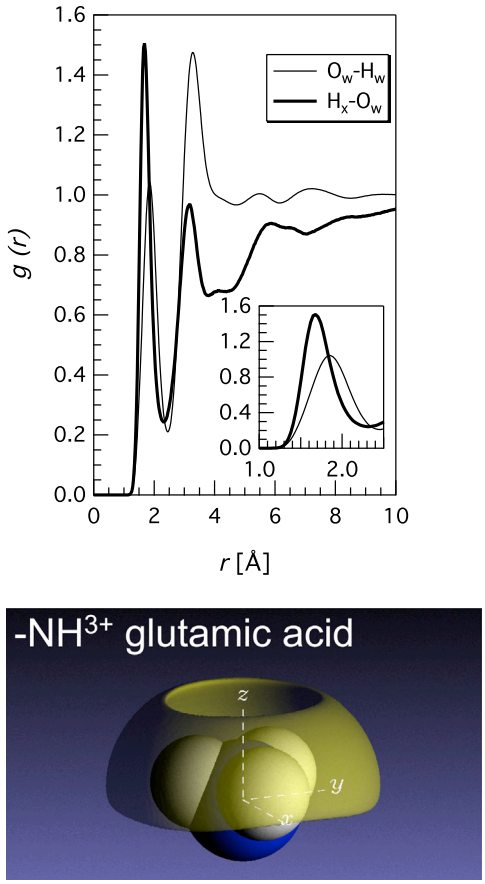

FIGURE 7 Top panel: site-site radial distribution function of water oxygen, O_w, around the hydrogens of the amine group on the glutamic acid, H_x (*thick solid line*). For the sake of comparison, the H_w-O_w is also plotted as a thin solid line. The first peak, usually taken as the signature of the H-bond, is clearly shifted to smaller distances for H_x-O_w, suggesting the presence of shorter and possibly stronger H-bonds between water and H_x sites of glutathione. Notice the slope, because of excluded volume effects, of the plotted RDF. Bottom panel: spatial density functions (SDF) showing the distribution of water molecules around the -NH^{3+} group on glutamic acid, see Fig. 1. The yellow shaded areas represents regions where there is a probability of finding a water molecule at a distance range 1 to 3.57 Å from the central nitrogen atom. This distance range corresponds to the first coordination shell of the N-O_w RDF (data not shown). The plotted SDFs show 70% of the water molecules within the ranges indicated. To see this figure in color, go online.

The reduced intensity of the hydrogen bond peak is immediately noticeable, that this peak is slightly shifted to larger distances suggests long, and possibly weaker, hydrogen bonds in comparison with pure water. The second shell (peak centered at ~ 4 Å), is also shifted to larger distances and much less defined, compared with pure water. Water coordination number around the -SH group of cysteine is unexpectedly small (0.64, see Table 1), given its ability to potentially act as a hydrogen bond donor and its position along the peptide chain favoring contact with the solvent. These observation could be rationalized as follows. The low affinity for water of the cysteine -SH group could be crucial in the oxidation/reduction mechanism of

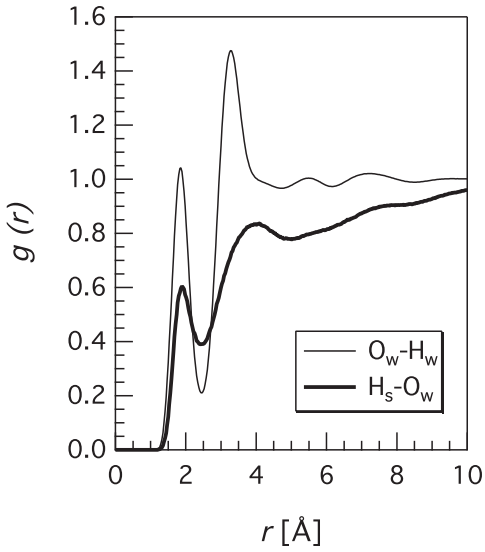

FIGURE 8 Site-site radial distribution function of water oxygen, O_w, around the hydrogen of the -SH group on cysteine, H_s (*thick solid line*). For the sake of comparison, the H_w-O_w is also plotted (*thin solid line*). The first peak, usually taken as the signature of the H-bond, is clearly reduced in amplitude and slightly shifted to larger distances for H_x-O_w, indicating a relatively low affinity for water of this highly reactive group of glutathione. The sloping behavior of the H_x-O_w RDF can be attributed to the presence of excluded volume effects.

glutathione: the conversion between GSH and GSSG requires a low energy barrier to be overcome. A strongly hydrogen bound water molecule on the -SH group is clearly not compatible with such a mechanism. Importantly, the low affinity of water for the -SH group observed here cannot be considered as concentration dependent, as there is an abundance of water molecules given the rather low concentration of the GSH solution examined. In addition, the -SH group will be deprotonated at pH $\not\geq$ 9 (30), thus indicating that the absence of a strong hydrogen bonding between the thiol group and a water molecule is not because of the low pH of the GSH solution examined in the present study. The absence of a strongly bound water molecule at the thiol group, again, is likely because of the issue of solvent accessibility of specific peptide sites. In the case of the -SH group we have a specific peptide group that is largely accessible to water (in the absence of steric hinderance due to neighboring groups), yet it shows a low affinity for water. This is also consistent with previous analysis of water molecule locations in protein crystallographic structures where it was suggested that sulfur containing groups were likely to be the least hydrophilic of all of the charged groups present on a protein surface (5). The different hydration shells of the carboxylate group determined for glutamic acid and glycine, along with the poor hydrogen bonding shown by the -SH group, point to water having a role in dictating both structural and functional properties of glutathione, as well as, by extension, on the surfaces of other proteins and peptides in solution.

CONCLUSIONS

We have used a combination of neutron diffraction experiments with isotopic substitution and computer simulation to study the water-glutathione interactions at the atomic scale, a relatively recent addition to the biophysical toolkit. Using this approach, possible connections between the hydration shells around specific sites of glutathione, an important intracellular antioxidant, have been determined. We have found that the highly reactive -SH group of the cysteine peptide has a rather low affinity for water, in keeping with previous analysis of water in protein crystal structures (5), despite its ability to act as a hydrogen bond donor. The hydration of this thiol group is crucial for the reaction leading to the oxidized form of glutathione, as an hydrogen bonded water molecule must be displaced from the -SH site to make a S-S bond with a second glutathione molecule. Equally, as cystine residues have an important role in the formation and stabilization of fully folded proteins in solution (33), the data here might give some future clues as to why S-S bonds form or break very readily between cystine residues in the presence of water, given that the -SH group is relatively underhydrated compared with the carboxylate and amide groups in GSH in solution.

Although it has been previously predicted from crystallographic data that carboxylate groups are the most hydrophilic groups on the surfaces on proteins (5), interestingly we have also found that the two (chemically identical) carboxylate groups on the glutamic acid and glycine residues have quite distinct hydration shells, differing both with respect to the number of water molecules and their spatial distribution around these groups. This finding indicates different solvent accessibility for the $-CO_2^-$ groups, depending on their location on the tripeptide and perhaps identity of the neighboring atoms. The different $-CO_2^-$ hydration shells may provide a way for water to "identify" specific peptide sites, and this ability might play a role in the early stages of protein folding, protein-ligand interactions, and a variety of other biophysical phenomena.

SUPPORTING MATERIAL

One figure, two tables, and References (34–37) are available at http://www.biophysj.org/biophysj/supplemental/S0006-3495(14)00186-6.

We acknowledge the skillful expertise and useful discussions with Dr. S. E. Pagnotta.

This work has been performed within the Agreement No.01/9001 between CCLRC and CNR, concerning collaboration in scientific research at the spallation neutron source ISIS and with partial financial support of CNR.

REFERENCES

1. Rupley, J. A., and G. Careri. 1991. Protein hydration and function. *Adv. Protein Chem.* 41:37–172.

2. Ball, P. 2008. Water as an active constituent in cell biology. *Chem. Rev.* 108:74–108.
3. Bernini, A., O. Spiga, …, N. Niccolai. 2011. Hydration studies on the archaeal protein Sso7d using NMR measurements and MD simulations. *BMC Struct. Biol.* 11:44.
4. Walsh, S. T. R., R. P. Cheng, …, W. F. DeGrado. 2003. The hydration of amides in helices; a comprehensive picture from molecular dynamics, IR, and NMR. *Protein Sci.* 12:520–531.
5. Kuhn, L. A., C. A. Swanson, …, E. D. Getzoff. 1995. Atomic and residue hydrophilicity in the context of folded protein structures. *Proteins.* 23:536–547.
6. Baron, R., and J. A. McCammon. 2013. Molecular recognition and ligand association. *Annu. Rev. Phys. Chem.* 64:151–175.
7. Hanson, W. M., S. A. Beeser, …, D. P. Goldenberg. 2003. Identification of a residue critical for maintaining the functional conformation of BPTI. *J. Mol. Biol.* 333:425–441.
8. McLain, S. E., A. K. Soper, and A. Watts. 2006. Structural studies on the hydration of L-glutamic acid in solution. *J. Phys. Chem. B.* 110:21251–21258.
9. McLain, S. E., A. K. Soper, …, A. Watts. 2007. Structure and hydration of L-proline in aqueous solutions. *J. Phys. Chem. B.* 111:4568–4580.
10. McLain, S. E., A. K. Soper, and A. Watts. 2008. Water structure around dipeptides in aqueous solutions. *Eur. Biophys. J.* 37:647–655.
11. Rhys, N. H., A. K. Soper, and L. Dougan. 2012. The hydrogen-bonding ability of the amino acid glutamine revealed by neutron diffraction experiments. *J. Phys. Chem. B.* 116:13308–13319.
12. Malardier-Jugroot, C., D. T. Bowron, …, T. Head-Gordon. 2010. Structure and water dynamics of aqueous peptide solutions in the presence of co-solvents. *Phys. Chem. Chem. Phys.* 12:382–392.
13. Merzel, F., and J. C. Smith. 2002. Is the first hydration shell of lysozyme of higher density than bulk water? *Proc. Natl. Acad. Sci. USA.* 99:5378–5383.
14. Mazza, M. G., K. Stokely, …, G. Franzese. 2011. More than one dynamic crossover in protein hydration water. *Proc. Natl. Acad. Sci. USA.* 108:19873–19878.
15. Botti, A., F. Bruni, …, A. K. Soper. 2004. Ions in water: the microscopic structure of concentrated NaOH solutions. *J. Chem. Phys.* 120:10154–10162.
16. Mancinelli, R., A. Botti, …, A. K. Soper. 2007. Perturbation of water structure due to monovalent ions in solution. *Phys. Chem. Chem. Phys.* 9:2959–2967.
17. Mancinelli, R., A. Botti, …, A. K. Soper. 2007. Hydration of sodium, potassium, and chloride ions in solution and the concept of structure maker/breaker. *J. Phys. Chem. B.* 111:13570–13577.
18. Bruni, F., S. Imberti, …, M. A. Ricci. 2012. Aqueous solutions of divalent chlorides: ions hydration shell and water structure. *J. Chem. Phys.* 136:064520.
19. Giustarini, D., A. Milzani, …, I. Dalle-Donne. 2005. S-nitrosation versus S-glutathionylation of protein sulfhydryl groups by S-nitrosoglutathione. *Antioxid. Redox Signal.* 7:930–939.
20. Sies, H., and T. P. Akerboom. 1984. Glutathione disulfide (GSSG) efflux from cells and tissues. *Methods Enzymol.* 105:445–451.
21. Soper, A. K., and D. K. Hyer. 1989. Future perspectives for liquids and amorphous materials diffraction at ISIS. *Proc. Conf. Advanced Neutron Sources*. D. K. Hyer, editor. 97:353–365.
22. http://www.disordmat.moonfruit.com.
23. Soper, A. K. 2011. GudrunN and GudrunX: programs for correcting raw neutron and X-ray diffraction data to differential scattering cross section. *Rutherford Appleton Laboratory Technical Report.* RAL-TR-2011-013.
24. Sears, V. F. 1992. Neutron scattering lengths and cross sections. *Neutron News.* 3:26–37.
25. Soper, A. K. 1996. Empirical potential Monte Carlo simulation of fluid structure. *Chem. Phys.* 202:295–306.
26. Soper, A. K. 1998. Determination of the orientational pair correlation function of a molecular liquid from diffraction data. *J. Mol. Liq.* 78:179–200.
27. Soper, A. K. 2005. Partial structure factors from disordered materials diffraction data: an approach using empirical potential structure refinement. *Phys. Rev. B.* 72:104204.
28. Soper, A. K. 2007. On the uniqueness of structure extracted from diffraction experiments on liquids and glasses. *J. Phys. Condens. Matter.* 19:415108.
29. Soper, A. K. 2007. Joint structure refinement of x-ray and neutron diffraction data on disordered materials: application to liquid water. *J. Phys. Condens. Matter.* 19:335206.
30. Rabenstein, D. L. 1973. Nuclear magnetic resonance studies of the acid-base chemistry of amino acids and peptides. Microscopic ionization constants of glutathione and methylmercury-complexed glutathione. *J. Am. Chem. Soc.* 95:2797–2803.
31. Soper, A. K. 2013. The radial distribution functions of water as derived from radiation total scattering experiments: is there anything we can say for sure? *ISRN Phys. Chem.* 2013:279463. http://dx.doi.org/10.1155/2013/279463.
32. Corridoni, T., R. Mancinelli, …, F. Bruni. 2011. Viscosity of aqueous solutions and local microscopic structure. *J. Phys. Chem. B.* 115:14008–14013.
33. Anfinsen, C. B. 1973. Principles that govern the folding of protein chains. *Science.* 181:223–230.
34. Berendsen, H. J. C., J. R. Grigera, and T. P. Straatsma. 1987. The missing term in effective pair potentials. *J. Phys. Chem.* 91:6269–6271.
35. Jorgensen, W. L., and J. Tirado-Rives. 1988. The OPLS [optimized potentials for liquid simulations] potential functions for proteins, energy minimizations for crystals of cyclic peptides and crambin. *J. Am. Chem. Soc.* 110:1657–1666.
36. Mancinelli, R., A. Sodo, …, A. K. Soper. 2009. Influence of concentration and anion size on hydration of H^+ ions and water structure. *J. Phys. Chem. B.* 113:4075–4081.
37. Hummer, G., D. M. Soumpasis, and M. Neumann. 1994. Computer simulation of aqueous Na-Cl electrolytes. *J. Phys. Condens. Matter.* 6:A141–A144.